RESTRICTED INVESTIGATION REPORT 1230R

CSIRO

INSTITUTE OF EARTH RESOURCES

DIVISION OF MINERAL PHYSICS

VARIABILITY OF MAGNETIC PROPERTIES IN THE CLEVELAND TIN MINE, TASMANIA

D.A. CLARK

P.O. Box 136,
NORTH RYDE, NSW
AUSTRALIA 2113

JUNE, 1981

RESTRICTED INVESTIGATION REPORT 1230

VARIABILITY OF MAGNETIC PROPERTIES IN THE CLEVELAND TIN MINE, TASMANIA

D.A. CLARK

CSIRO Division of Mineral Chemistry,
P.O. Box 136,
North Ryde, NSW. 2113
AUSTRALIA

JUNE, 1981.

TABLE OF CONTENTS

LIST OF TABLES

LIST OF FIGURES

1. INTRODUCTION

The work described in this report was carried out as part of the CSIRO-AMIRA rock magnetism project no. 78/P96.

At the instigation of Mr. J. Silic of Aberfoyle NL access to the Cleveland Tin mine at Luina was arranged and a sampling programme carried out by D.A. Clark and B.J.J. Embleton of the CSIRO. The aim of this study is to provide a case history of the variability of magnetic properties within a pyrrhotitic ore body and to gain an idea of the amount of sampling required to adequately characterise a deposit of this sort. It is important to know, for instance, approximately how many samples are needed to provide useful input to magnetic interpretation.

2. REMANENCE AND SUSCEPTIBILITY

Because many areas of the mine could not be sampled safely, underground sampling was restricted to 24 Level and part of 20 Level. Eighteen block samples of pyrrhotitic ore and two of barren shale were collected from 24 Level, 4 ore samples were taken from 20 Level (in both cases from B Lens) and a further 4 ore samples were collected at the surface on Hall's workings.

In 24 Level sampling was carried out along the full extent of the drive from footwall and hangingwall faces enabling determination of along-strike variations and expression of zoning in the magnetic properties.

The NRM intensities, susceptibilities and Koenigsberger ratios of the 24 Level samples are given in Table 1 and the same parameters for the 20 Level and surface samples are quoted in Table 2.

As expected, the shale samples are only weakly magnetic. The massive ore samples are variably magnetic with emu susceptibilities ranging from 660×10^{-6} to $25{,}160 \times 10^{-6}$. For the ore samples Koenigsberger ratios are predominantly greater than unity and for 24 Level the unweighted average Q value is 2.4. Therefore we can expect that remanence dominates the induced magnetisation in this ore body, as found commonly in sulphide ores. The representative Q value for this deposit should be

somewhat lower than 2.4 as the more magnetic samples tend to have lower Koenigsberger ratios.

There is no significant variation between J and k values of samples taken from the footwall and hanging wall, so there is no evidence in the magnetic measurements for zoning of the ore body parallel to the lithological layering. Definite trends are apparent along strike, however. As we move inwards from the ends of the drive the k and J values increase, reflecting the trend towards more massive ore.

Susceptibility values, which are mainly determined by the proportion of monoclinic pyrrhotitic in the sample, show no clear trend up-dip, as k values from 20 Level and the surface are consistent with those found at 24 Level. The anomalously high NRM intensities of the surface samples are reflected in the very high, but variable, Koenigsberger ratios which suggest these rocks are lightning struck.

All samples were oriented using magnetic compass only and in the case of the underground samples the strike directions were confirmed by sighting along the drive. It was felt that the strikes were accurate to $\pm 10^{o}$. The magnetisation of the rocks underground is not so high that very large declination anomalies are expected. On the surface, however, the intense NRMs make the magnetic orientations highly suspect and the sample mean NRM directions are very scattered, whereas those of the underground samples are well grouped.

The NRM directions of the shale samples are consistent with the ore sample directions, so all 24 underground sample mean directions can be combined to give a formation mean direction which is roughly NE and steeply upwards. (Figure 1).

Mean NRM direction = $(32^{o}, -75^{o})$

$(N = 24, R = 21.72, \alpha_{95} = 10^{o})$

AF and thermal cleaning reveal the presence of only a single component of magnetisation. Similar NRM directions were found by Falvey (1966).

This direction is only 7^{o} from the present field (12^{o}, -71^{o}) and may therefore be a viscous magnetisation acquired very recently. Consistent with a viscous origin, the magnetisation is very soft to AF demagnetisation, with median destructive field 20 Oersteds. However, the blocking temperatures of the NRM are predominantly greater than 200^{o}C, which is surprisingly high for a VRM, particularly one which must have been acquired in less than 10,000 years to have failed to average secular variation and therefore reflect only the anomalously steep field of the very recent past at this locality. The magnetisation is not consistent with a VRM acquired over a significant proportion of the Brunhes normal polarity interval (the last 700,000 years) as the direction is significantly steeper than the dipole field direction at this locality, namely (0^{o}, -61^{o}).

This line of argument suggests that the magnetisation may be more ancient. Because of the low Curie temperature of pyrrhotite, about 320^{o}C, it is relatively easily reset by heating and the magnetisation could well reflect a low-grade thermal event. The palaeomagnetic pole calculated from the mean direction is (62^{o}S 112^{o}E) which, by comparison with the apparent polar wander track relative to Australia for the Mesozoic and Tertiary given by Embleton and McElhinny (1981), suggests an age of about 50 m.y. for the magnetisation. This magnetisation may have been "frozen in" during cooling associated with uplift and removal of overburden. In the igneous and sedimentary rocks of S.E. Australia a ubiquitous 90 my overprint has been found and is thought to be due to uplift and cooling of the continental margin during initial opening of the Tasman Sea. (Schmidt and Embleton, 1981).

Whatever the origin of the magnetisation, its direction is sufficiently close to present field that induction could safely be assumed in modelling, providing the effective susceptibility of the model was enhanced to account for the contribution of the remanence.

3. STATISTICAL ASPECTS

The values of the parameters k, J and Q and their logarithms were grouped in classes of equal width and the frequency distributions calculated. The frequency histograms for k, J and Q are shown in Figure 2.

Overall it can be seen that J has a symmetric distribution whereas k and to a lesser extent, Q have skewed distributions with a prominent tail for high values. These histograms are suggestive of normal and log-normal distributions respectively. The fit of the observed distributions to these theoretical distributions was tested by plotting cumulative frequencies against class midpoint on probability paper, both for the parameters and their logarithms. If this procedure produces a straight line the quantity plotted is normally distributed, and statistical estimation problems are reduced to standard procedures.

The results show that J, log k and log Q are approximately normally distributed, i.e. k and Q can be fitted by a log-normal distribution. Estimation from log-normal distributions is more complicated than from normal distributions, but the theory is nevertheless well understood (Aitchison and Brown, 1957). The basic problem is that the arithmetic mean of the sample values, whilst an unbiassed estimate of the true mean, is not robust. This is reflected in the well-known fact that with skewed distributions, like that of k here, the sample mean is likely to be unduly influenced by one or two very high values, causing it frequently to overestimate the true mean. The effect is negligible for very large samples, but for the number of measurements here the minimum variance unbiassed estimator of the mean should be used.

To calculate the best estimate of the true mean susceptibility of the ore body, based on the 26 ore samples, the following procedure is necessary:

(i) For each sample ln k is taken and the mean m and variance V of the logarithms calculated.

(ii) The best estimate of the true mean is exp(m) $\gamma(V)$ where $\gamma(V)$ is Sichel's t-estimator, which is tabulated in David (1977, pp 20-21).

Applying this:-

$N = 26$, Arithmetic mean $k = 5,954$ s.d. = 5,463

$M = 8.317$, $V = 0.8254$

$\therefore\ e^m\ \gamma(V) = 4,093 \times 1.5008 = 6,143$

Since the standard error = $5,463/\sqrt{26} = 1,072$ the sample arithmetic mean and the best estimate of the true mean differ by only 18% of the standard error and there is little to choose between the estimators in this case.

Note also the sample median value is 4,130 which is very close to the value estimated by the geometric mean = $e^m = 4,093$.

Since the remanence direction for the undisturbed underground samples is virtually constant, the representative remanent intensity can be calculated from the individual sample intensities, without regard to remanence directions. Because the intensities can be taken as belonging to a normal population, the appropriate estimate of the mean value is simply the arithmetic mean of the sample values:

For the 22 underground ore samples we have:-

$\bar{J} = 7,070 \pm 1,440$ (s.d. = 6,774)

The effective Koenigsberger ratio can then be estimated from the mean remanent intensity and susceptibility values:

$Q = \bar{J} / (\bar{k} \times 0.625) = 1.84 \pm 0.49$

where the error is calculated assuming relative error equals the square root of the sum of the squares of the relative errors in $\bar{J}$ and $\bar{k}$.

This estimate of Q is less than the arithmetic mean of Q values for the individual samples(2.36)because the samples with the highest Koenigsberger ratios are generally less magnetic than average. It seems the most appropriate value of Q to represent the relative contributions of remanence and induction throughout the whole body is the estimate based on $\bar{J}$ and $\bar{k}$.

Because in this case remanent and induced magnetisations are essentially parallel it is valid to assume induction in modelling taking the effective susceptibility $k' = \bar{k} \ (1 + Q) = 2.84 \ \bar{k}$.

In recent times an advanced theory of regionalised variables has been developed for purposes of geostatistical ore reserve estimation. Techniques are available which give best estimates of average ore grades, total tonnages, risks and profitability etc. (David, 1977). In the case of estimation of average grade the technique is known as kriging.

Petrophysical parameters such as specific gravity, magnetic susceptibility and NRM intensity can also be regarded as regionalised variables and geostatistical methods can be applied. The key concept in geostatistics is that of the variogram, which is an inverse measure of the correlation between sample values as a function of the separation of the samples. In the one-dimensional case the variogram is defined by:-

$$2\gamma(h) = [1/N(h)] \ \Sigma \ [Z(x_i) - Z(x_i + h)]^2$$

where the Z(x) are sample values, N(h) is the number of samples separated by h, and the summation is from i = 1 to i = N(h).

Because correlation between samples generally decreases with separation, $\gamma(h)$ generally increases with h. The range of a variogram is the distance over which $\gamma(h)$ increases before reaching a plateau and therefore measures the zone of influence of a sample. Samples separated by more than the range are uncorrelated.

If $\gamma(0)$ is non-zero, the variogram is said to exhibit a nugget effect. Nugget effects reflect a component of random variation in the

variable at the scale of sampling. If the variogram is simply a plateau it is called pure nugget effect type, and samples are uncorrelated whatever their separation. On the other hand, continuity in the deposit is reflected in gradual increase of $\gamma(h)$. The plateau value beyond the range of influence is known as the sill.

In Figure 3 the variograms for k and J are shown. There is some scatter but the data can be quite well fitted by a spherical model (David, 1977, p. 122) for k and a linear model for J.

The susceptibility variogram has negligible nugget effect and a range of 15 metres. The equation fitted to the data points by eye is:-

$$\gamma(h) = 17.5\ [1.5\ (^{h}/15) - 0.5\ (^{h}/15)^{3}]\ ,\ h < 15$$
$$\gamma(h) = 17.5,\quad h > 15$$

For J there is a small nugget effect and no apparent zone of influence. The variogram can be fitted by:-

$$\gamma(h) = 0.75h + 5.25$$

From these variograms the best linear unbiased estimator of the average values can be calculated by kriging. In practice a computer is required, using one of the now freely available programmes for this purpose (e.g. David, 1977). As the geostatistical approach should now be used for routine ore reserve calculations, it is highly desirable that mine managers have access to geostatistical packages. These programmes could then be usefully applied to petrophysical studies.

The fact that the variograms shown in Figure 3 can be constructed implies that the sampling on 24 Level was sufficient to define the gross structure of the magnetic parameters of this lens. This is also borne out by the comparison of various estimates of mean values, which suggest that approximately 20 samples, of volume approximately 100 cm^3, distributed over a strike length of 70 metres is sufficient to estimate mean values to within 20% (which is the appproximate standard error for both k and J). Values of k for 8 further samples distributed over a dip distance of about 500 metres (24 Level to Hall's workings) are consistent with the

distribution of values found on 24 Level, which confirms the assumption that this lens, at least, has been well characterised by the sampling. Had only one quarter of the number of samples been taken, the relative error would double to approximately 40%, which is probably unacceptable. If only 10 samples had been collected from 24 Level, it is probably that well-defined variograms could not have been calculated.

4. MAGNETIC FABRIC

The susceptibility of the ore samples is generally quite anisotropic, as evidenced by the anisotropy data given in Tables 3 and 4. Furthermore the magnetic fabric is consistent from specimen to specimen within a sample, and there is definite evidence of a preferred orientation of magnetic minerals throughout the body.

Thermognetic (k-T) analysis of a Cleveland ore sample reveals the presence of only a single magnetic mineral - monoclinic pyrrhotite with a Curie temperature of 320°C (Figure 4). Therefore the magnetic fabric arises from preferred crystallographic orientation of pyrrhotite, which reflects a deformational event. This does not necessarily imply that formation of the pyrrhotite pre-dates the deformation, which in this area is associated with the Devonian Taberraberan orogeny. It is conceivable that the pyrrhotite fabric is mimetic and merely reflects the deformational fabric of the silicate minerals. However, the high anisotropy values observed are hard to explain as a result of mimetic fabric.

In Tables 3 and 4 the following parameters are listed:

Anisotropy A = maximum susceptibility/minimum susceptibility
Lineation L = maximum susceptibility/intermediate susceptibility
Foliation F = intermediate susceptibility/minimum susceptibility
Prolateness P = L/F ($P < 1$: predominantly oblate (planar) fabric
$P > 1$: predominantly prolate (linear) fabric)

The value of A determines the maximum possible deflection of induced magnetisation away from the ambient field direction towards the easy magnetisation direction (maximum susceptibility direction). The overall anisotropy of the ore samples is probably less than 40% ($A < 1.4$)

and this corresponds to a maximum deflection of 10^{o}. If the ambient field lies close to an easy direction of magnetisation, as is the case here because of the near vertical magnetic foliation plane, then the deflection will be much less. Therefore susceptibility anisotropy should not significantly affect magnetic interpretation in this case.

In Table 5 the magnetic lineation directions and foliation poles are given. The 24 Level samples exhibit a very consistent fabric with well-grouped foliation poles plunging shallowly to the southwest (Figure 5). The lineations are randomly dispersed within the corresponding foliation plane, which has northeast strikes and dips very steeply to the northwest. Consistent with this planar parallel fabric, the susceptibility ellipsoids of individual samples are predominantly oblate ($P < 1$). The magnetic foliation plane corresponds to the preferred orientation of the basal planes of pyrrhotite crystals and in this case is approximately parallel to the bedding. X-ray goniometry work on a few ore samples from the mine is described by Falvey (1966) and the results indicate preferred alignment of pyrrhotite C-axes in close agreement with the mean foliation pole shown in Figure 5. The magnetic method is a far more convenient and efficient technique for elucidating pyrrhotite fabric.

Most other studies on magnetic fabrics associated with pyrrhotite have found the magnetic foliation pole to correspond to the axis of maximum compression. The foliation plane then coincides with the cleavage, if any. Magnetic lineations parallel the direction of maximum extension, and are probably due to shape anisotropy of deformed pyrrhotite grains with maximum susceptibility along the elongation direction within the basal plane. Together with the high degree of preferred orientation found in these samples, this suggests the observed fabric is deformational and that the magnetic foliation represents an incipient cleavage, which is sub-parallel to the bedding.

The 4 samples from 20 Level, on the other hand, have prolate susceptibility ellipsoids, suggestive of extension, and randomly scattered foliation poles. The average lineation appears to plunge shallowly to the NNW. The reason for the difference between the fabrics found at 24 Level and 20 Level is not clear, but may be related to relative proximity to a fold hinge, with consequent variation of the strain ellipsoid.

5. CONCLUSIONS

(i) The distributions of susceptibility and NRM intensity values within B lens to the Cleveland ore body appear to have been fairly well characterised by the level of sampling carried out (total of 28 small block samples over a strike length of 70 metres, up-dip distance of 500m, lens thickness 10 metres).

(ii) Calculation of variograms for k and J on 24 Level suggest the applicability of modern geostatistical methods to estimation of average susceptibility and remanence.

(iii) The magnetisation of this body is dominated by remanence which is directed sub-parallel to the Earth's present field. Induction could be assumed in modelling, provided the model susceptibility is enhanced to account for the contribution of remanence. Susceptibility anisotropy is not significant for interpretation.

(iv) The NRM of the pyrrhotite ore may be of recent viscous origin, or it may reflect a thermal event in the early Tertiary. The relatively high stability of the NRM to thermal demagnetisation suggests a thermal origin for the magnetisation, possibly 50 m.y. ago.

(v) Strong preferred orientation of pyrrhototite grains is revealed by susceptibility anisotropy measurements. The magnetic foliation plane strikes approximately NE, dipping very steeply to the NW, and is considered to represent an analogue of cleavage.

6. REFERENCES

J. Aitchison and J.A.C. Brown (1957). "The Lognormal Distribution", C.U.P.

M. David (1977), "Geostatistical Ore Reserve Estimation" Elsevier.

B.J.J. Embleton and M.W. McElhinny (1981), "Marine magnetic anomalies, palaeomagnetism and the drift history of Gondwanaland", submitted to Nature.

D. Falvey (1966) "The interpretation of geophysical surveys at the Cleveland Mine, Tasmania", Hons. thesis (unpubl.), University of Sydney

P.W. Schmidt and B.J.J. Embleton (1981), "Magnetic overprinting in south-eastern Australia and the thermal history of its rifted margin", J. Geophys. Res. (in press).

FIGURE CAPTIONS

Figure 1 Stereographic plot of NRM directions. The primitive represents the present horizontal. Open symbols denote upward-pointing directions.

Figure 2 Frequency histograms for k, J and Q.

Figure 3 Variograms for k and J.

Figure 4 Low-field (k-T) thermomagnetic curve for Cleveland ore sample. The susceptibility drops very rapidly immediately below the Curie temperature of 320°C. The irreversibility of the curve on cooling indicates chemical change in the sample after heating to 350°C.

Figure 5 Magnetic fabric of samples from 24 Level. Equal area lower hemisphere projection. The primitive represents the present horizontal.

TABLE 1. SUSCEPTIBILITY AND NRM INTENSITY (24 LEVEL, B LENS)

Sample	N	NRM intensity (microgauss)	Emu susceptibility ($\times 10^6$)	Koenigsberger ratio (H=0.625 Oersteds)
1 (shale)	9	11	60	0.29
2	6	2,010	660	4.90
3	10	8,470	7,310	1.85
4	17	9,590	7,190	2.13
5	8	6,760	4,040	2.68
6	8	7,680	2,990	4.11
7	5	9,830	6,590	2.39
8	6	15,950	13,330	1.91
9	24	10,670	8,670	1.97
10	18	3,530	3,060	1.85
11	25	6,014	25,160	0.57
12	8	6,340	3,480	2.91
13	23	6,010	2,540	3.79
14	7	5,690	2,700	3.37
15	4	6,920	4,530	2.44
16	14	3,040	4,220	1.15
17 (shale)	7	12	53	0.36
18	8	470	650	1.14
19	10	2,560	1,400	2.91
20	22	1,170	1,780	1.05

N = no. of speciments drilled from block sample

For the 18 ore samples the following relationships hold:
(i) Susceptibilities are approximately log-normally distributed (i.e. log k is normal) with arithmetic mean 5,570, geometric mean 3,740, median 3,760, mode 2,750, standard deviation 5,840, standard error 1,380.
(ii) NRM intensities are approximately normally distributed with arithmetric mean 6,420, standard deviation 3,920 and standard error 920.
(iii) Koenigsberger ratios are approximately log-normally distributed with arithmetic mean 2.40, standard deviation 1.14, standard error 0.27, geometric mean 2.12, median 2.17, mode 1.75.

TABLE 2. SUSCEPTIBILITY AND NRM INTENSITY (20 LEVEL AND SURFACE)

20 Level, B Lens

Sample	N	NRM Intensity (microgauss)	Emu susceptibility ($\times 10^6$)	Koenigsberger ratio (H = 0.625 Oersteds)
1	4	610	1,050	0.93
2	4	4,410	3,240	2.18
3	2	2,710	2,000	2.17
4	5	32,120	15,400	3.34

Hall's open-cut

1	5	464,600	6,170	120
2	4	566,200	9,070	100
3	15	33,670	9,480	5.7
4	15	63,290	8,100	12.5

TABLE 3. SUSCEPTIBILITY ANISOTROPY PARAMETERS (24 LEVEL, B LENS)

Sample	N	Anisotropy	Lineation	Foliation	Prolateness
1	8	1.09	1.03	1.06	0.97
2	3	1.21	1.06	1.14	0.94
3	9	1.56	1.13	1.37	0.86
4	16	1.31	1.09	1.22	0.90
5	8	1.29	1.06	1.21	0.89
6	6	1.13	1.05	1.08	0.98
7	4	1.18	1.08	1.10	0.98
8	5	1.41	1.11	1.26	0.90
9	24	1.29	1.11	1.16	0.97
10	18	1.21	1.17	1.04	1.13
11	25	1.24	1.07	1.15	0.94
12	7	1.11	1.07	1.05	1.02
13	23	1.38	1.15	1.20	0.97
14	7	1.29	1.11	1.16	0.98
15	4	1.37	1.11	1.25	0.89
16	14	1.31	1.07	1.21	0.90
17	6	1.08	1.04	1.04	1.00
18	8	1.47	1.09	1.35	0.86
19	7	1.28	1.08	1.18	0.93
20	22	1.55	1.10	1.39	0.91

Ore samples (N = 18): $\bar{A} = 1.31 \pm 0.03$ (SD = 0.13)
$\bar{L} = 1.10 \pm 0.01$ (SD = 0.03)
$\bar{F} = 1.20 \pm 0.02$ (SD = 0.10)
$\bar{P} = 0.94 \pm 0.02$ (SD = 0.07)

TABLE 4. SUSCEPTIBILITY ANISOTROPY PARAMETERS (20 LEVEL, B LENS)

Sample	N	Anisotropy	Lineation	Foliation	Prolateness
1	4	1.74	1.33	1.29	1.02
2	4	1.39	1.11	1.26	0.93
3	2	1.28	1.17	1.09	1.07
4	5	1.45	1.28	1.14	1.13

$\bar{A} = 1.47 \pm 0.10$ (SD = 0.20)
$\bar{L} = 1.22 \pm 0.05$ (SD = 0.10)
$\bar{F} = 1.20 \pm 0.05$ (SD = 0.10)
$\bar{P} = 1.04 \pm 0.04$ (SD = 0.08)

TABLE 5. MAGNETIC FABRIC

24 Level, B Lens

Sample	Lineation (α_{95})	Foliation Pole (α_{95})	Remarks
1	(20^{o}, $+78^{o}$) (12^{o})	(149^{o}, $+7^{o}$) (9^{o})	
2	(55^{o}, $+56^{o}$) (39^{o})	(185^{o}, $+22^{o}$) (23^{o})	
3	--	--	No distinct fabric
4	--	(158^{o}, $+14^{o}$) (9^{o})	Maximum susceptibility axes dispersed about girdle
5	(76^{o}, -17^{o}) (15^{o})	(164^{o}, $+7^{o}$) (23^{o})	
6	(59^{o}, -12^{o}) (14^{o})	(135^{o}, $+47^{o}$) (17^{o})	
7	--	--	No distinct fabric
8	--	(158^{o}, -43^{o}) (40^{o})	Maximum susceptibility axes dispersed about girdle
9	(18^{o}, 0^{o}) (9^{o})	(108^{o}, $+11^{o}$) (10^{o})	
10	(42^{o}, -14^{o}) (6^{o})	(141^{o}, -1^{o}) (13^{o})	
11	(91^{o}, -57^{o}) (11^{o})	--	Minimum susceptibility axes either NE or SE with shallow dips
12	(38^{o}, $+20^{o}$) (29^{o})	(144^{o}, $+20^{o}$) (32^{o})	
13	(43^{o}, -18^{o}) (11^{o})	(135^{o}, $+5^{o}$) (11^{o})	
14	--	(63^{o}, $+12^{o}$) (30^{o})	Maximum susceptibility axes dispersed about girdle
15	--	(109^{o}, $+19^{o}$) (19^{o})	"

TABLE 5 Cont'd

Sample	Lineation	Foliation Pole	Remarks
16	$(116^{\circ}, -19^{\circ})$ (21°)	$(112^{\circ}, +70^{\circ})$ (15°)	
17	$(66^{\circ}, -32^{\circ})$ (24°)	$(149^{\circ}, +2^{\circ})$ (24°)	
18	--	$(121^{\circ}, -8^{\circ})$ (25°)	Maximum susceptibility axes dispersed about girdle
19	$(332^{\circ}, +61^{\circ})$ (32°)	$(157^{\circ}, +25^{\circ})$ (40°)	
20	$(46^{\circ}, -12^{\circ})$ (18°)	$(125^{\circ}, +16^{\circ})$ (17°)	
	20 Level, B Lens		
1	$(321^{\circ}, +49^{\circ})$ (17°)	--	Minimum susceptibility axes dispersed about girdle
2	$(302^{\circ}, +43^{\circ})$ (29°)	--	"
3	$(323^{\circ}, +7^{\circ})$ (27°)	--	"
4	$(19^{\circ}, -3^{\circ})$ (41°)	--	"

24 Level: Mean foliation pole $(141^{\circ}, +14^{\circ})$, $\alpha_{95} = 15^{\circ}$
N = 16, K = 7.0

$\therefore$ Magnetic foliation plane has approximately NE strike and dips at 76° to the NW.

Directions are quoted in the form (declination, inclination) with declination measured positive clockwise from north, and inclination defined as positive downwards.

α_{95} is the radius of the error circle about the mean direction, at the 95% confidence level.

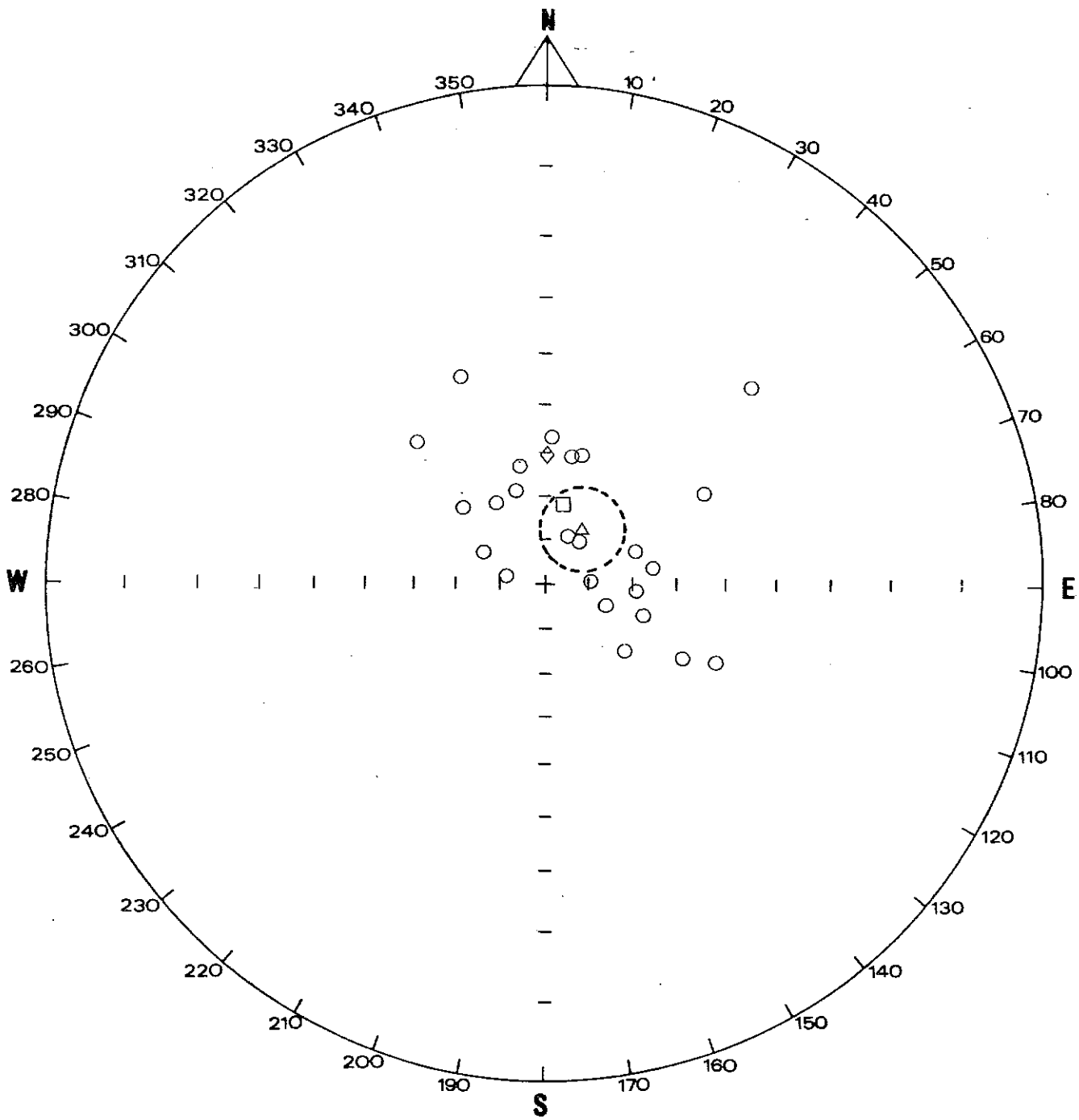

○ Sample mean NRM directions

△ Mean NRM direction and cone of confidence

□ Present field direction

◇ Dipole field direction

FIG. 1

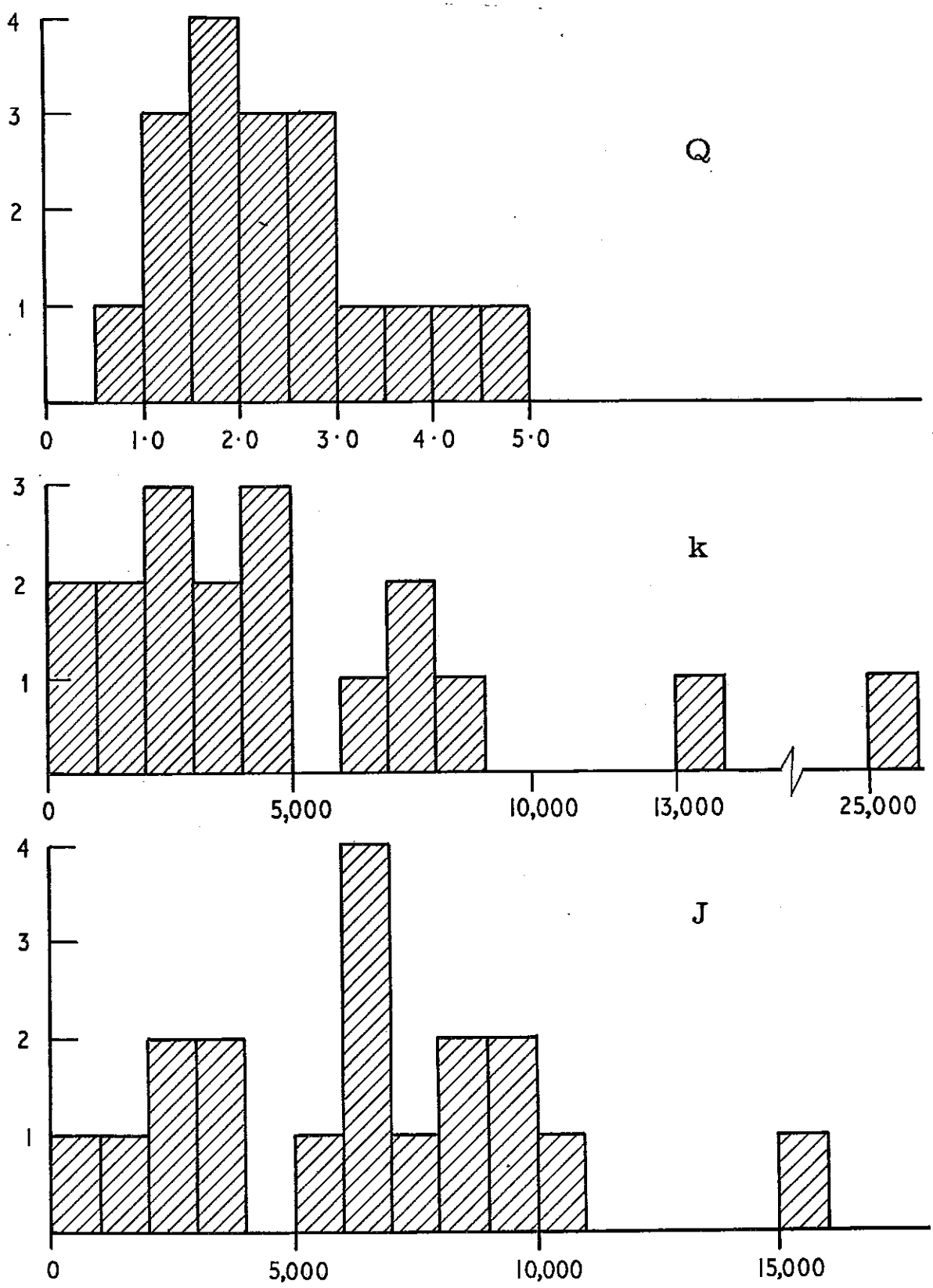
4
3
2
1
Q
0
1·0
2·0
3·0
4·0
5·0
3
2
1
k
0
5,000
10,000
13,000
25,000
4
3
2
1
J
0
5,000
10,000
15,000

FIG. 2

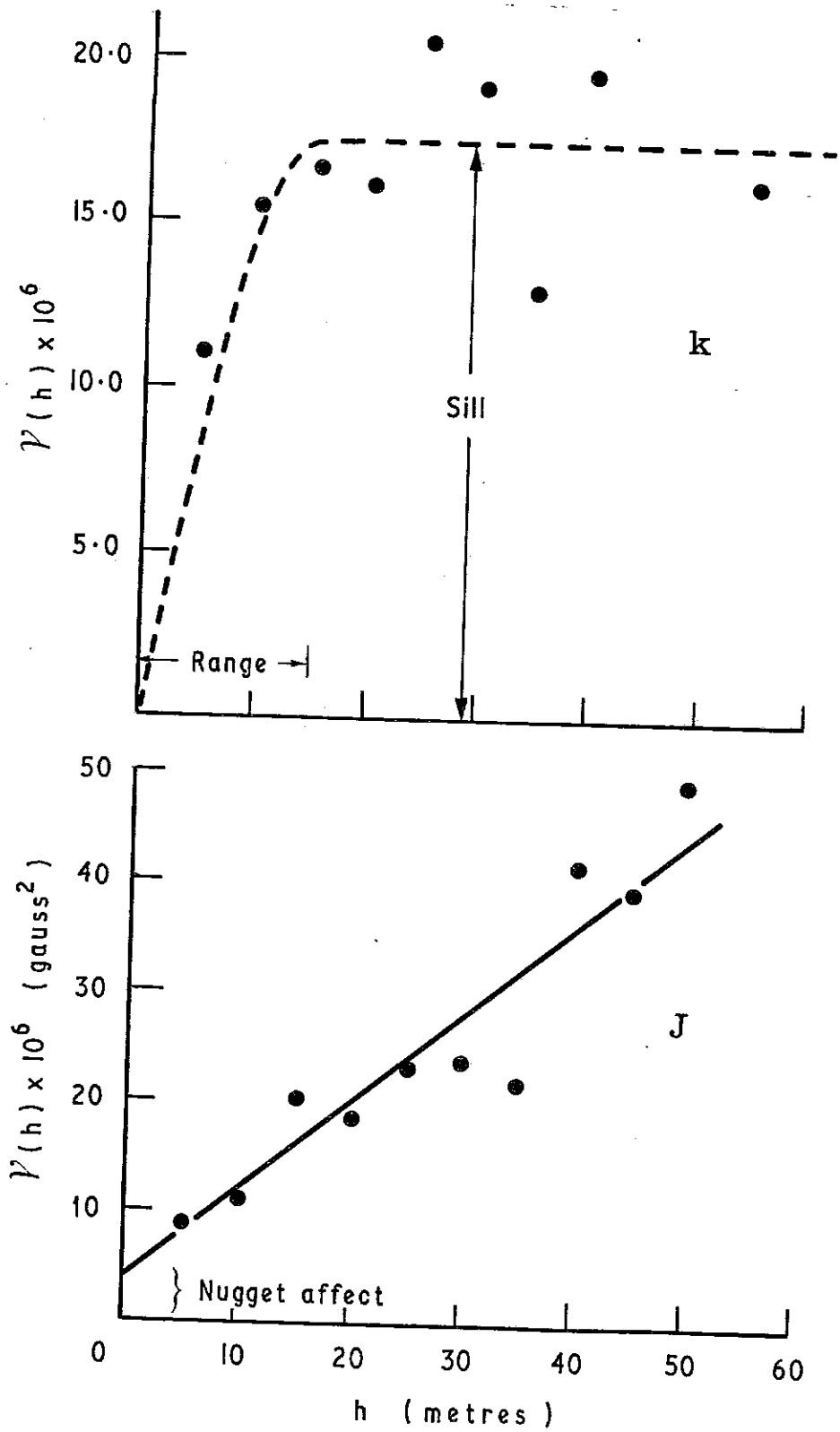
20·0
15·0
10·0
5·0
γ(h) x 10^6
k
Sill
Range
50
40
30
20
10
0
γ(h) x 10^6 (gauss^2)
J
Nugget affect
10
20
30
40
50
60
h (metres)

FIG. 3

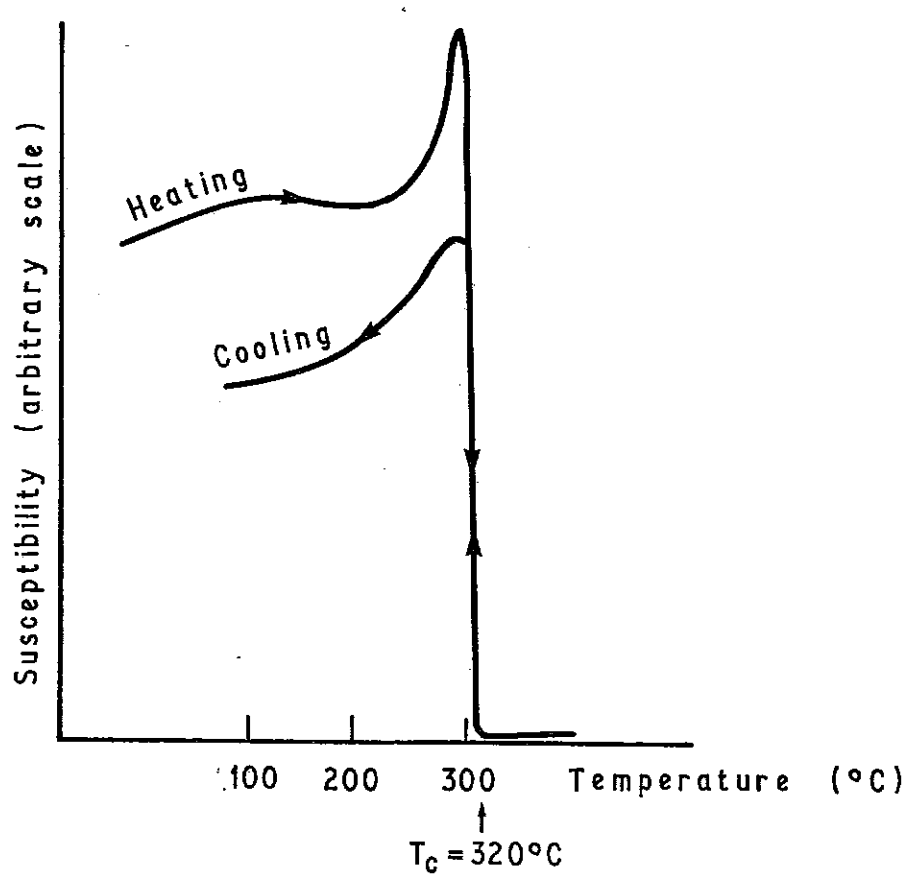
Susceptibility (arbitrary scale)
Heating
Cooling
100
200
300
Temperature (°C)
$T_c = 320°C$

FIG. 4

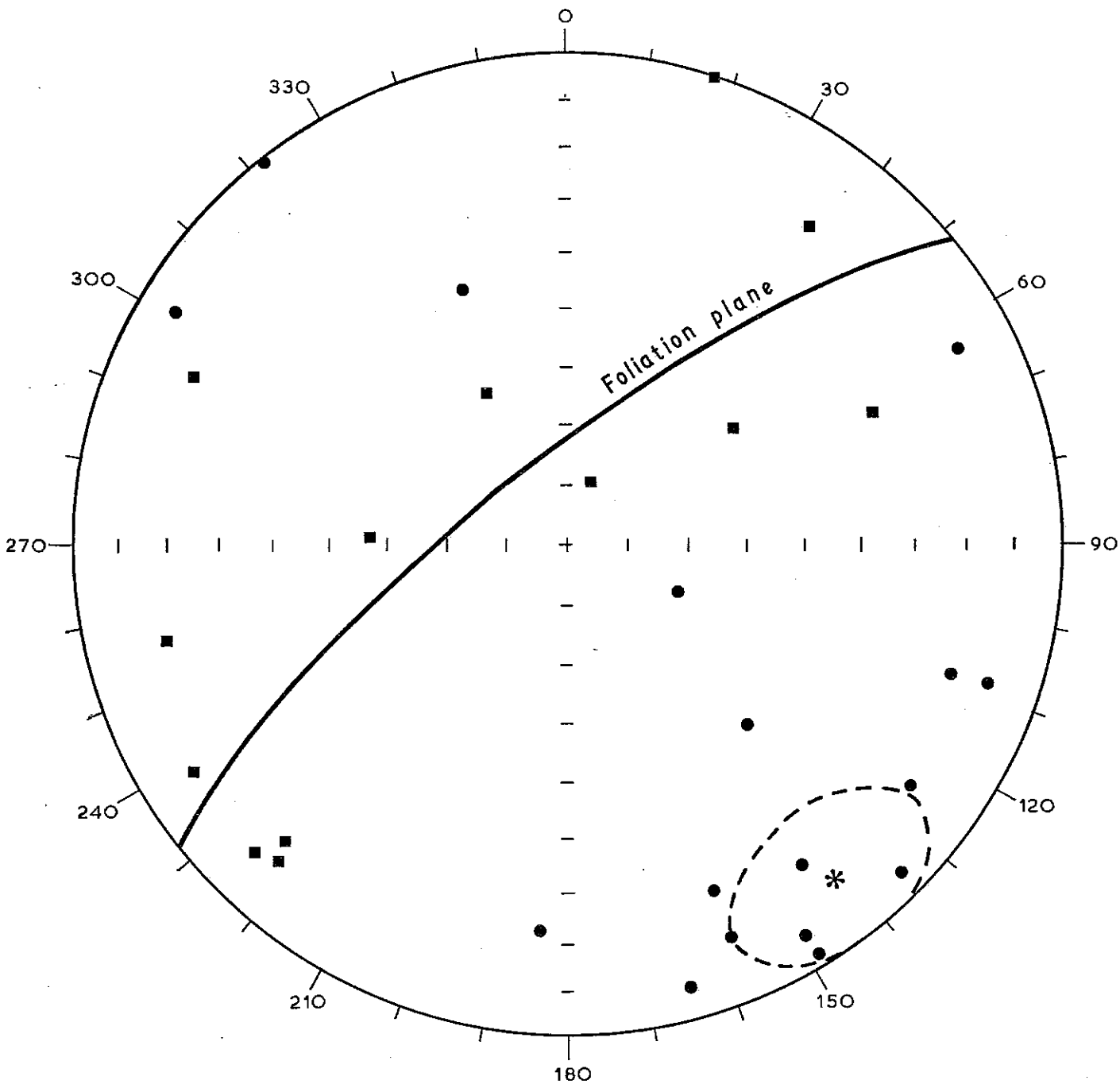

■ Lineations ● Foliation poles

✻ Mean foliation pole and error oval

FIG. 5